View metadata, citation and similar papers at core.ac.uk
brought to you by CORE
provided by NASA Technical Reports Server

QUANTIFICATION OF CROSS-COUPLING AND MOTION FEEDTHROUGH FOR MULTIAXIS CONTROLLERS USED IN AN AIR COMBAT FLYING TASK

Wayne F. Jewell
Systems Technology, Inc.
2672 Bayshore-Frontage Road, Suite 505
Mountain View, California 94035

Kevin D. Citurs
McDonnell Aircraft Company
Box 516, Bldg. 32, Level 2, Post 280
St. Louis, Missouri 63166

SUMMARY

A real-time piloted simulation of an air-to-air combat flying task using a "wings-level-turn" aircraft and various novel controllers was conducted at the U. S. Air Force Flight Dynamics Laboratory (USAFFDL), Wright-Patterson Air Force Base, Ohio, on the Large Amplitude Multimode Aerospace Research Simulator (LAMARS). One objective of this on-going Air Force-sponsored research is to quantify how the pilot interacts with the controllers and control modes, including:

1. Controller versus aircraft response (i.e., pilot control strategy and describing functions).

2. Proprioceptive cross-coupling among axes of the controllers.

3. Biodynamic cross-coupling between the aircraft motions and the controllers.

In order to aid in identifying the items listed above, both the target aircraft and the LAMARS motion system were disturbed with qausi-random sums-of-sinusoids. Since the disturbances were separated in frequency, spectral analysis techniques could be used to identify the three items listed above. This paper presents the results of the spectral analysis of controller motions from the two-axis side stick, a twist grip mounted on the side stick, a thumb button mounted on the side stick, and conventional rudder pedals. Conclusions and recommendations for further research are also presented.

INTRODUCTION

The results presented in this paper are based on work performed under a U. S. Air Force contract to develop design criteria and gather appropriate substantiating data for cockpit control devices for use with six-degree-of-freedom (6-DOF) uncoupled aircraft. The purpose of this study was to insure compatibility among the pilot, the control device(s), and the aircraft response which will allow efficient utilization of the 6-DOF capability. The prime contractor was the McDonnell Aircraft Company, and

Systems Technology, Inc., (STI) acted as a subcontractor for the work reported herein.

The project evaluated many different tasks, uncoupled aircraft motions, and controller configurations. A complete description of the overall project can be found in Refs. 1 and 2. This paper will be restricted to an air-to-air combat task using an aircraft with "wings-level-turn" (WLT) capability and three different cockpit controllers which can be used with the WLT mode.

DESCRIPTION OF THE CONTROL TASK

The control task is depicted in the block diagram of Fig. 1. For the experiments analyzed herein, the pilot was instructed to track the target motions (i.e., keep the target in the pipper) using the WLT controller (δ_{WLT}) and to keep the wings level using the roll controller (δ_P).

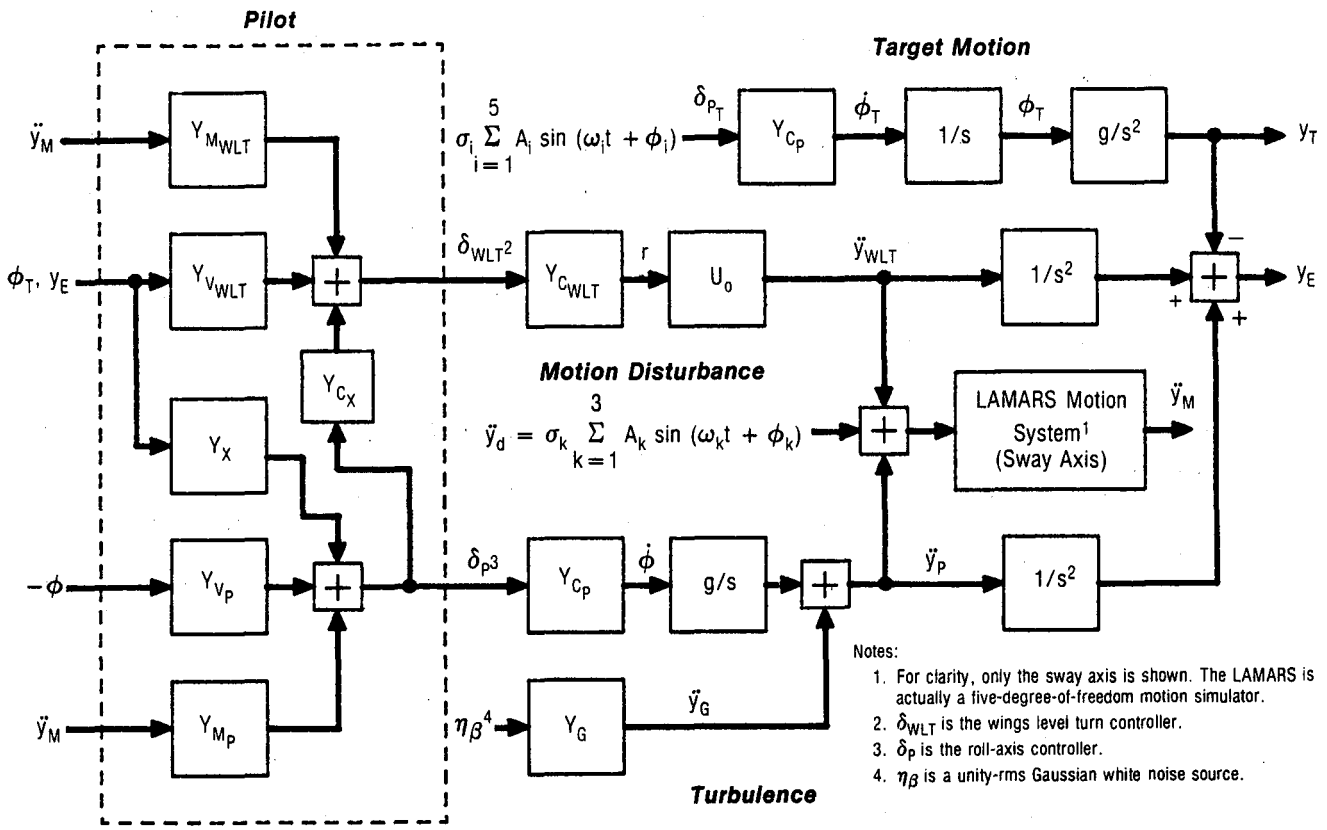

Figure 1. Functional Block Diagram of Pilot Control Task, Target Motion, and Motion Disturbance for Air-to-Air Tracking Task

Using the WLT mode (also referred to as a flat turn mode), the pilot can turn the aircraft without creating a side slip and without changing the roll attitude. The appropriate transfer functions for the WLT mode are shown below.

$$\frac{r}{\delta_{WLT}} = \frac{1.0}{0.5s + 1.0} N_{\delta_{WLT}} \equiv Y_{C_{WLT}} \tag{1}$$

$$\frac{\beta}{\delta_{WLT}} = 0 \tag{2}$$

$$\frac{\phi}{\delta_{WLT}} = 0 \tag{3}$$

$$n_y = \frac{U}{g} r \tag{4}$$

Where $N\delta_{WLT}$ was used to set the maximum control power. For the experiments described herein, the control power was $n_{y_{max}} = 1.0$ g at the specified maximum control force.

The appropriate transfer functions for the roll mode are shown below:

$$\frac{p}{\delta_P} = \frac{L_{\delta_P}}{0.35s + 1} \equiv Y_{C_P} \tag{5}$$

$$\frac{\beta}{\delta_P} = 0 \tag{6}$$

Where $L\delta_P$ was used to set the maximum control power. For the experiments described herein, the control power was $p_{max} = 150$ deg/sec at maximum side stick deflection. The roll side stick sensitivity was 12.5 deg/sec per pound of δ_P.

The pilot's control actions shown in Fig. 1 are represented by a sum of linear feedbacks proportional to the aircraft's bank angle (ϕ), the target's bank angle (ϕ_T), the difference between the aircraft and the target aircraft, the pipper error (y_E), and the lateral acceleration ($\ddot{y}_M$). The y_E and ϕ feedbacks are represented by $Y_{V_{WLT}}$ and Y_{V_P}, respectively. The crossfeed term, Y_X, is in Fig. 1, because some pilots might "cheat" by using the roll controller, δ_P, to chase the target. The target bank angle is fed back through $Y_{V_{WLT}}$, because it is possible to use ϕ_T to

anticipate the target motion and thus generate lead. Controller cross-coupling is represented by the term Y_{C_X}. The coupling is shown with the roll controller summing with the WLT controller, but the opposite direction is also possible. "Biodynamic" feedthrough is represented by the terms $Y_{M_{WLT}}$ and Y_{M_P}, which represent how the aircraft's lateral acceleration, $\ddot{y}$, affect the pilot's controls, δ_{WLT} and δ_P, respectively.

The aircraft is being disturbed by two noise sources, as shown in Fig. 1. Dryden turbulence is injected into the equations of motion, while the motion disturbance is injected directly into the LAMARS motion system; thus, it is uncorrelated with the aircraft motion. The purpose of the Dryden turbulence is to add realism to the simulation. The transfer function for the Dryden turbulence is:

$$Y_G \equiv \frac{\ddot{y}_G}{\eta_\beta} = \frac{\omega_{dr}^2 \, n_{y_\beta} (g/U) \, \sigma_{v_g} (3R_\beta)^{1/2}}{[\zeta_{dr}; \omega_{dr}] \; (s + 1.5R_\beta)} \tag{7}$$

where $R_\beta = U/1750$ rad/sec, $\sigma_{v_g} = 3.0$ fps, $\omega_{dr} = 4.47$ rad/sec, $\zeta_{dr} = 0.68$, $n_{y_\beta} = -5.73$ g/rad, and η_β is a unity amplitude Gaussian noise source.

The purpose of the motion disturbance is to quantify how aircraft accelerations will affect the use of the various controllers. Since the motion disturbance, $\ddot{y}_d$, is formed by a sum of three discrete sine waves, it is possible to "trace" the signals through to the controllers, δ_{WLT} and δ_P. Thus the terms $Y_{M_{WLT}}$ and Y_{M_P} could theoretically be identified. The amplitudes, A_k, and frequencies, ω_k, used to form $\ddot{y}_d$ are listed in Table 1. The phase angle, ϕ_k, were randomly chosen from run to run. The magnitude of the motion disturbance was subjectively set such that the motion could be felt but was not a dominant effect. The subject test pilots were not informed of the motion disturbance.

The target aircraft motions, ϕ_T and Y_T shown in Fig. 1, were formed by using a sum of five sine waves as the input to the roll controller. The target motions were recorded on magnetic tape and then played back during realtime simulation. The phasing between the sine waves, ϕ_i, was set such that a zero-mean process for ϕ_T was obtained, and the target aircraft was constrained to remain in the same vertical plane. The magnitude of the input, σ_i, was set such that the root-mean-square (rms) bank angle of the target aircraft was approximately 15 deg. The amplitudes, A_i, and frequencies, ω_i, used to form δ_{P_T} are shown in Table 2. Because the power in the target motion exists at discrete frequencies, it is theoretically possible to identify the terms $Y_{V_{WLT}}$, Y_X, Y_{C_X}, and Y_{V_P}.

OBJECTIVES

The overall objective of the analysis contained herein is to quantify how the pilot interacts with the various novel controllers and control modes described herein, including:

TABLE 1. PARAMETERS USED TO FORM THE MOTION DISTURBANCE FUNCTION, $\ddot{y}_d$

k	A_k	N_k	ω_k	ϕ_k
(-)	(-)[3]	(cycles/T_y)[1]	(rad/sec)[1]	(rad)[2]
1	0.9698	9 (1.8 Hz)	11.310	--
2	0.7886	13 (2.6 Hz)	16.336	--
3	0.6610	19 (3.8 Hz)	23.876	--

Notes: (1) $\omega_k = 2\pi N_k/T_y$, T_y = 5 seconds

(2) The ϕ_k are random numbers computed at the beginning of a run. They are constant throughout a run.

(3) Amplitude shaping is based on first-order power spectra with a break frequency at 0.5 rad/sec and unity rms.

TABLE 2. PARAMETERS USED TO FORM THE TARGET MOTION FUNCTION, δ_{P_T}

i	A_i	N_i	ω_i	ϕ_i
(-)	(-)[3]	(cycles/T_T)[1]	(rad/sec)[1]	(rad)[2]
1	0.9328	4 (0.04 Hz)	0.2513	--
2	0.7838	10 (0.10 Hz)	0.6283	--
3	0.5825	30 (0.30 Hz)	1.885	--
4	0.3519	70 (0.70 Hz)	4.398	--
5	0.2290	150 (1.5 Hz)	9.425	--

Notes: (1) $\omega_i = 2\pi N_i/T_T$, T_T = 100 seconds

(2) The ϕ_i are set such that the target bank angle, δ_T, is a zero-mean process (see Fig. 1)

(3) Amplitude shaping is based on first-order power spectra with a break frequency at 1.5 rad/sec and unity rms.

1. Controller versus aircraft response behavior (e.g., pilot control strategy and describing functions). This can be quantified by the terms $Y_{V_{WLT}}$, Y_X, and Y_{V_P} in Fig. 1.

2. Proprioceptive cross-coupling among the axes of the controllers (e.g., roll commands due to twist grip deflections). This can be quantified by the term Y_{C_X} in Fig. 1.

3. Aircraft motion-to-controller coupling ("biodynamic cross-coupling"). This can be quantified by identifying the terms $Y_{M_{WLT}}$ and Y_{M_P} in Fig. 1.

ANALYTICAL TECHNIQUES

As mentioned above, it is theoretically possible to identify the terms in Fig. 1 by using describing function and/or time domain analysis techniques. Due to time and resource constraints and the intensive level of computations required, however, we were unable to complete the analysis. Instead, the next section presents the power spectra and power fractions of the roll and WLT controllers for a selected group of runs. By examining the power spectra, we can tell if the disturbances are present in the controllers; that is, if the pilot can be modeled as a linear system as shown in Fig. 1, then all of the power in δ_{WLT} would be at the target frequencies, ω_i. Furthermore, if the pilot did not use the roll controller to track the target, then the power in δ_P would be "white" (i.e., because the Dryden turbulence is shaped white noise). If biodynamic coupling exists, then there will also be power in δ_P and/or δ_{WLT} at the motion disturbance frequencies, ω_k.

SOME EXAMPLE RESULTS

The analysis contained below compares the data from three different types of controllers used to perform an air-to-air tracking task using a wings-level-turn (WLT) mode. The three controllers were:

1. Conventional rudder pedals, δ_{RP}.

2. An isotonic twist grip, δ_{TG}. This was the twist axis of a right-handed side-stick controller.

3. The thumb button controller, δ_{TBC}, mounted on the right-handed side-stick controller.

Table 3 is a summary of the runs analyzed. Note that the maneuver gradient was held constant for each of the WLT controllers while either the dead band (DB) for the twist grip or thumb button or breakout force (BO) for the rudder pedals was varied. As shown in Table 3, the pilot-opinion rating (POR) varied from 2 to 5 as a function of either deadband or breakout force.

TABLE 3. SUMMARY OF RUNS ANALYZED

Run No.	WLT Controller	Controller Characteristics	POR	Pilot Comments	Analysis Comments
3145	Rudder Pedals*	4.0 lb BO**	2	None	Very little motion feedthrough to δ_{RP}. Lots to δ_p. Some possible crosscoupling.
3137		7.0 lb BO	3	"Not bad"	No motion feedthrough to δ_{RP}. Still lots to δ_p. Some possible crosscoupling.
3141		15.0 lb BO	3	"Feet got tired"	Same as above.
3143		25.0 lb BO	5	"Too much pedal to start and stop"	Strange looking spectra for δ_{RP}. Note jump in CH from 3 to 5.
3081	Twist Grip#	0.5 in-lb DB	2	"No problem"	Lots of motion feedthrough. Definite cross-coupling at ω = 1.8 rad/sec.
3084		2.7 in-lb DB	3	"Has a little lag"	Same as above.
3092		4.8 in-lb DB	4	None	Motion feedthrough and crosscoupling reduced.
3086		9.6 in-lb DB	5	"Too much delay"	Definite crosscoupling. No motion feedthrough.
3188	Thumb Button##	0.05 lb DB	3	"Little loose"	Lots of crosscoupling and motion feedthrough.
3190		0.50 lb DB	3	"Good"	Reduced coupling and motion feedthrough.
3194		1.0 lb DB**	3	"Had to work a little harder than normal"	Further reduction in coupling and motion feedthrough. Note that CH remains 3.
3192		1.5 lb DB	5	"Bad"	Increased use of δ_p. Note that CH jumped to 5.

*Rudder pedals had 2 inches of travel and a maneuver gradient of 40 lb/g.
**DB = deadband, BO = breakout.
#Twist grip had a maneuver gradient of 24 in-lb/g and was the rotational axis on the two-axis right-handed side stick.
##Thumb button has a maneuver gradient of 3.3 lb/g and was mounted on the two-axis right-handed side stick.

Figures 2 through 4 contain power spectra and power fraction plots of the roll controller and the appropriate WLT controller. The power fraction is a unique way to visualize the spectral distribution in a signal. It is defined as follows:

$$PF(\omega) = \frac{1}{\sigma_x^2} \int_0^{\omega} \Phi_{xx}(\omega)dx$$

Note that $\sigma_x^2 \equiv PF(\omega = \infty)$, thus $PF(\omega)$ is a fraction from 0.0 to 1.0. The unique feature of the power fraction is that it defines the bandwidth of a signal in terms of a percentage (e.g., 90 percent of the power is below 5.2 rad/sec).

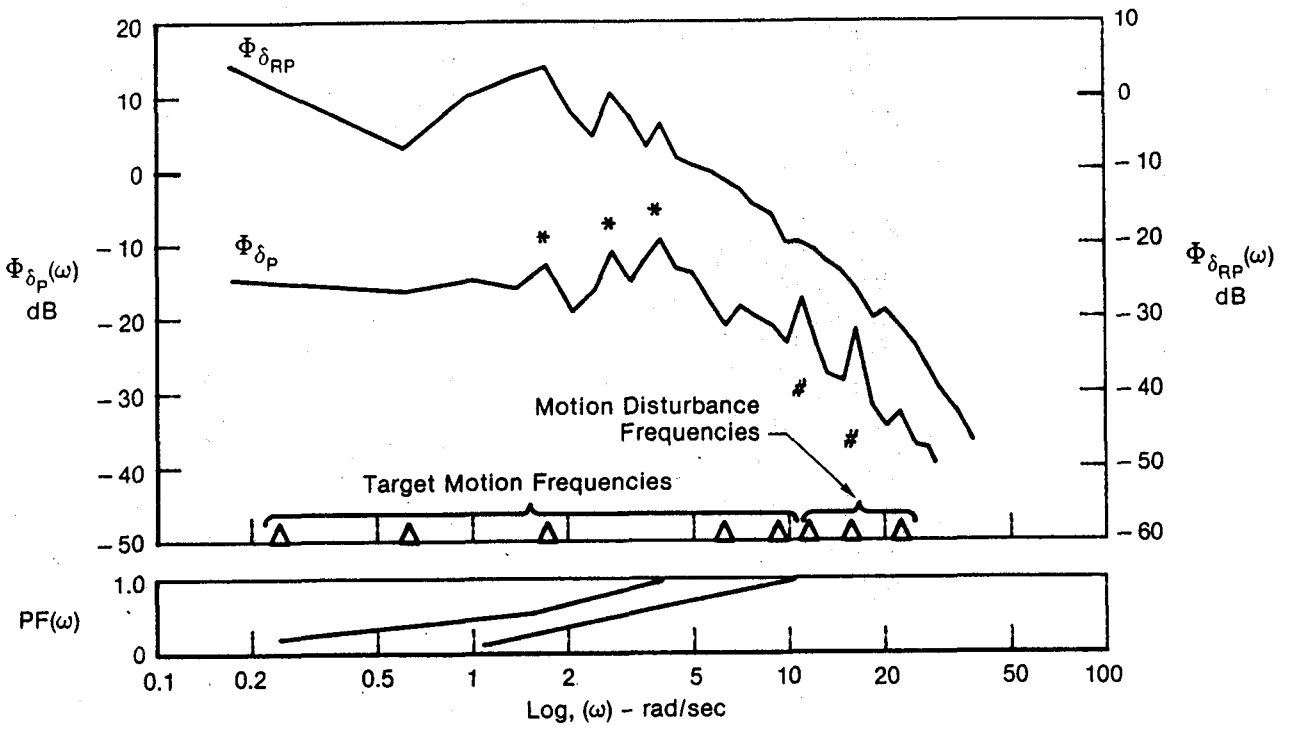

Notes:

* Crosscoupling between controllers suggested by the line spectra in Φ_{δ_P} and $\Phi_{\delta_{RP}}$ at the same frequency. However, at the target disturbance frequency, this could also be due to the pilot using δ_P to "chase" the target (even though he was instructed not to do so).

\# Motion feedthrough evidenced by line spectra at motion disturbance frequencies.

Figure 2. Power Spectra [$\Phi(\omega)$] and Power Fraction [$PF(\omega)$] for Wings Level Turn and Roll Control Inputs
Rudder Pedal, 2 in. Deflection; 7 lb Breakout;
40 lb/g Maneuver Gradient; Cooper-Harper Rating = 3

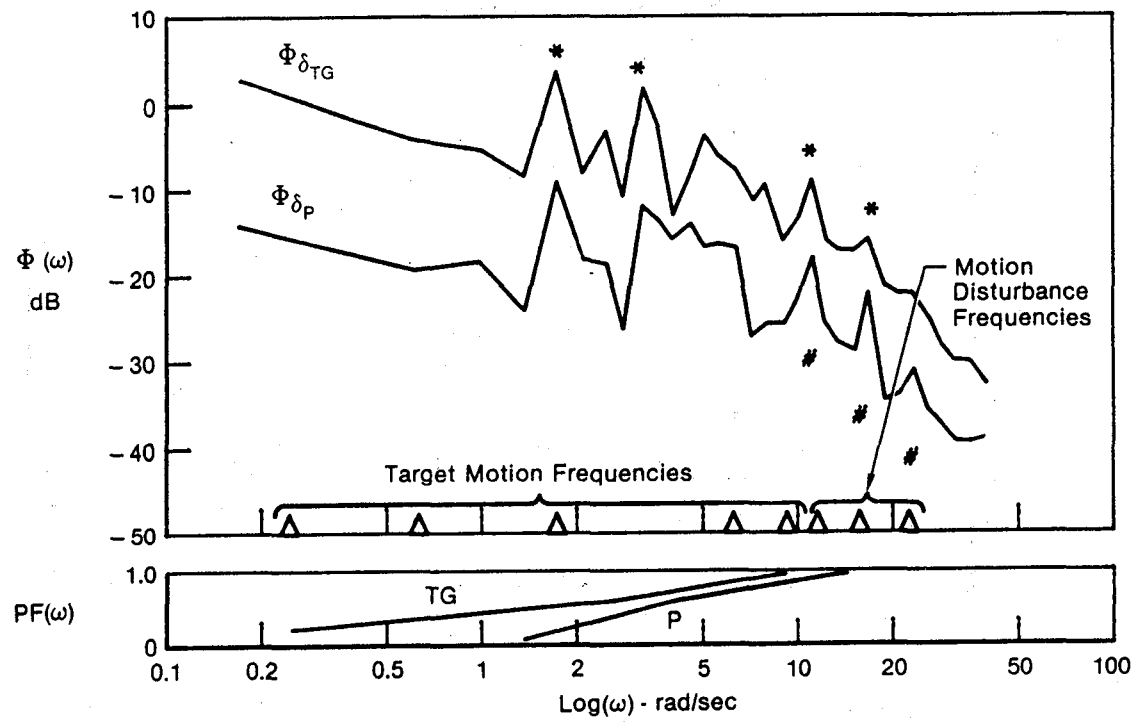

Notes:

* Crosscoupling between controllers suggested by the line spectra in Φ_{δ_P} and $\Phi_{\delta_{TG}}$ at the same frequency. However, at the target disturbance frequency, this could also be due to the pilot using δ_P to "chase" the target (even though he was instructed not to do so).

\# Motion feedthrough evidenced by line spectra at motion disturbance frequencies.

Figure 3. Power Spectra [Φ(ω)] and Power Fraction [PF(ω)] for Wings Level Turn and Roll Control Inputs Twist Grip Sidestick; 2.7 in-lb Deadband; 24 in-lb/g Maneuver Gradient; Cooper-Harper Rating = 3

The following observations were made after carefully examining these plots:

1. There are large amounts of motion feedthrough ("biodynamic coupling") to the roll controller (i.e., lateral side stick) for all runs. This is evidenced by the "line spectra" (i.e., the spikes for apparent discontinuities in the power spectra) at the motion disturbance frequencies. It is interesting to note that none of the pilots complained of motion-to-controller coupling. This is probably because the accelerations were small in amplitude and were masked by the Dryden turbulence. However, motion-to-controller coupling can have extremely detrimental effects in actual flight where the accelerations are much larger.

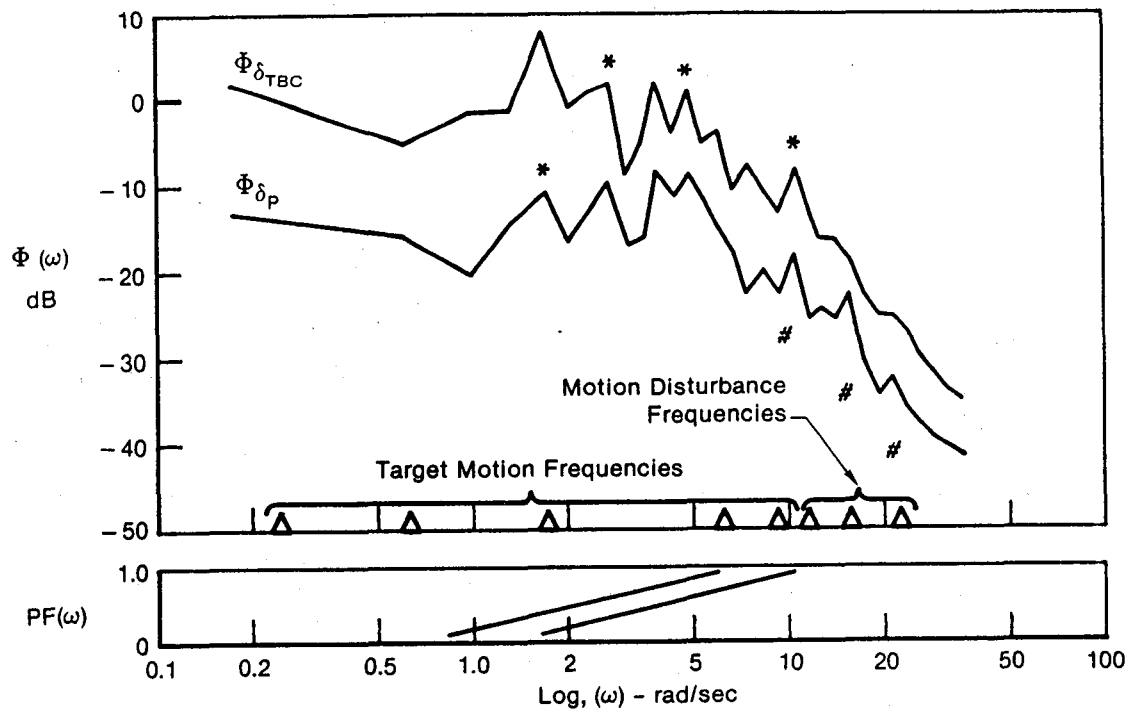

Notes:

* Crosscoupling between controllers suggested by the line spectra in Φ_{δ_P} and $\Phi_{\delta_{TBC}}$ at the same frequency. However, at the target disturbance frequency, this could also be due to the pilot using δ_P to "chase" the target (even though he was instructed not to do so).

\# Motion feedthrough evidenced by line spectra at motion disturbance frequencies.

Figure 4. Power Spectra [Φ(ω)] and Power Fraction [PF(ω)] for Wings Level Turn and Roll Control Inputs Thumb Button Controller; 0.05 lb Deadband; 3.3 lb/g Maneuver Gradient; Cooper-Harper Rating = 3

2. There is evidence of motion feedthrough on all of the WLT controllers, with most on the twist grip and the least on the rudder pedals. As the deadband is increased, the evidence of motion feedthrough is decreased.

3. There appears to be controller cross-coupling between the roll and WLT controllers for the twist grip and thumb button but very little for rudder pedals. This is evidenced by the line spectra in δ_P and δ_{WLT} at the same frequencies. This is especially true (and consistent) at the motion disturbance frequencies and makes sense, because the pilot must the grab the sidestick in order to use the twist grip or the thumb button but not to use the rudder pedals.

4. Note that the rudder pedals are the only controller for which clear line spectra do appear at the target disturbance frequencies and do not appear at the motion disturbance

frequencies. All of the other controllers (roll side stick, twist grip, and thumb button) exhibit line spectra at both disturbance frequency levels. Note also that, for the rudder pedal plots, line spectra do appear for the roll controller at the target disturbance frequencies. Since physical coupling is not possible between these controllers, the plots suggest that the pilot is either consciously or unconsciously using the roll controller to assist in chasing the target. It is probably a combination of both, as the coupling seems stronger in the twist grip and thumb button plots (i.e., the magnitudes of the spikes in the roll controller are larger) where proprioceptive coupling is possible.

5. Line spectra at all of the disturbance frequencies were not clearly or consistently observed (ω = 1.8 rad/sec is the only possible exception to this observation). This is probably due to nonlinearities in the pilot's control technique such as saturation (e.g., bang-bang control) or aperiodic sampling.

CONCLUSIONS AND RECOMMENDATIONS

Using spectral analysis techniques, it was possible to identify controller cross coupling for the air-to-air combat task described herein. However, because of the nature of the task, it was not possible to discern whether the coupling was proprioceptive (e.g., twisting the side stick to effect the wings-level-turn mode without affecting the roll controller) or whether the pilot was intentionally using both controllers to improve tracking performance. We recommend performing two additional tasks which will help to isolate the coupling effects:

- Track the target without the WLT controller. This will reveal how much roll control is being used when the pilot is not using the WLT controller.

- Track the target with the roll axis of the aircraft fixed (i.e., short the connection between δ_p and the roll axis equations of motion). Reduce the dead band on δ_p to zero, and measure the spectra of δ_p.

The first task would assist in giving the analyst a feel for what to expect in $\Phi_{\delta p}(\omega)$ for a pilot actively chasing the target with only the roll controller. The second task would yield spectra for the use of the WLT controller without roll axis chasing contamination. Some caution must be applied when using this task, however. Since there would be no penalty (i.e., roll response) for making roll inputs, the pilot might modify his technique to such an extent as to invalidate the spectra of δ_p. This effect could be minimized by providing the pilot with some form of feedback, other than roll response, to indicate when roll inputs are being made.

Spectral analysis of the controller signals also revealed large amounts of biodynamic coupling; that is, the aircraft accelerations were feeding through to the controllers by way of the pilot's limbs. Because the simulated accelerations are quite small relative to the real world, none of the subject pilots complained of motion feedthrough problems. We recommend that analytic techniques be used to predict the amount of acceleration to expect in real flight and how the accelerations will affect overall performance of the pilot-aircraft system. Existing tools such as Biodyn (Ref. 3) and USAM (Ref. 4) could be used to perform this task.

We also recommend a complete pilot-vehicle analysis. Using a loop structure like the one shown in Fig. 1, the closed-loop characteristics of the pilot-vehicle system could be predicted. The effects of cross coupling and motion feedthrough could be quantified.

REFERENCES

1. Citurs, Kevin D., Controller Requirements for Uncoupled Aircraft Motion. Volumes I and II of Final Report for Period August 1981 to April 1984, McDonnell Aircraft Company Report, April 1984, forthcoming as an AFML TR.

2. Citurs, Kevin D., "Controller Requirements for Uncoupled Aircraft Motion," to be presented at the 11th Annual Atmospheric Flight Mechanics Conference, Seattle, Washington, August 1984.

3. Magdaleno, Raymond E., and Henry R. Jex, Biodynamic Models for Effects of Low-Frequency Vibration on Performance, Systems Technology, Inc., Paper No. 307, presented at the Naval Biodynamics Laboratory Workshop on Research Methods in Human Motion and Vibration Studies, New Orleans, LA, September 16, 1981.

4. Teper, Gary L., The STI Library of Control System Design Programs, Systems Technology, Inc., Working Paper No. 407-1, February 11, 1974, Revised August 1976.